The Journal of Histochemistry & Cytochemistry

ARTICLE

Tubular Stress Proteins and Nitric Oxide Synthase Expression in Rat Kidney Exposed to Mercuric Chloride and Melatonin

Alessandra Stacchiotti, Francesca Ricci, Rita Rezzani, Giovanni Li Volti, Elisa Borsani, Antonio Lavazza, Rossella Bianchi, and Luigi Fabrizio Rodella

Division of Human Anatomy, Department of Biomedical Sciences and Biotechnology, University of Brescia, Brescia, Italy (AS,FR,RR,GLV,EB,RB,LFR), and Laboratory of Electron Microscopy, Istituto Zooprofilattico Sperimentale della Lombardia ed Emilia-Romagna, Brescia, Italy (AL)

SUMMARY Stress proteins such as HSP70 members (HSP72 and GRP75) and metallothionein (MT) protect the kidney against oxidative damage and harmful metals, whereas inducible nitric oxide synthase (iNOS) regulates tubular functions. A single dose of mercuric chloride ($HgCl_2$) can cause acute renal failure in rats, its main target being the proximal tubule. Oxidative damage has been proposed as one of its pathogenic mechanisms. In this study we tested whether melatonin (MEL), a powerful antioxidant compound, is effective against $HgCl_2$ nephrotoxicity. Rats were treated with saline, $HgCl_2$ (3.5 mg/kg), MEL (5 mg/kg), and MEL + $HgCl_2$ and examined after 24 hr for HSP72, GRP75, MT, and iNOS by immunohistochemistry and immunoblotting. Tubular effects of the treatment were then characterized by ultrastructure. In the $HgCl_2$ group, all markers were overexpressed in convoluted proximal tubules and sometimes in distal tubules. In the MEL + $HgCl_2$ group, GRP75 and iNOS decreased in convoluted and straight proximal tubules, whereas HSP72 and MT persisted more than the saline and MEL-only groups. Tubular damage and mitochondrial morphometry were improved by MEL pretreatment. In conclusion, the beneficial effect of MEL against $HgCl_2$ nephrotoxicity was outlined morphologically and by the reduction of the tubular expression of stress proteins and iNOS. These markers could represent sensitive recovery index against mercury damage. **(J Histochem Cytochem 54:1149–1157, 2006)**

CELLS AND ORGANISMS have developed a common extraordinary mechanism called the "stress proteins response" to resist a wide variety of stress (Kultz 2005). Stress proteins are universally conserved chaperones rapidly induced or overexpressed against adverse pathophysiological conditions (Beck et al. 2000). HSP72 is an inducible member of the multigene HSP70 family, located in the cytoplasm that maintains both cellular homeostasis and ATP levels (Mallouk et al. 1999). GRP75 is another member located in the inner mitochondrial membrane where it assembles and recovers respiratory enzymes damaged during oxidative stress (Wadhwa et al. 2002). Metallothioneins (MT) belong

to the "stress-specific stress proteins" that participate in the detoxification of heavy metals and oxygen free radicals (Sato and Kondoh 2002). MT is induced in the proximal tubules of kidneys exposed to mercuric chloride ($HgCl_2$), and its protective role has been confirmed in MT knockout mice in $HgCl_2$ nephrotoxicity experiments (Satoh et al. 1997; Yoshida et al. 2004).

Nitric oxide is a gas generated from L-arginine by nitric oxide synthase (NOS) that regulates glomerular hemodynamics, the release of sympathetic neurotransmitters, renin (Kone 2004), and tubular functions (Jarry et al. 2003). Its inducible isoform (iNOS) is calcium independent and exacerbates renal oxidative damage (Chatterjee et al. 2002).

The kidney is a favorite target for several pollutants (Van Vleet and Schnellmann 2003) due to its peculiar anatomical–physiological features, i.e., mainly large blood flow and enzymatic activity. $HgCl_2$ is an established nephrotoxicant in rats where it dose dependently affects the pars recta (S3 segment) of the proximal

tubules (Stacchiotti et al. 2003). Tubular necrosis, induced both in vitro and in vivo, has been attributed to oxidative damage (Aleo et al. 2002; Shimojo et al. 2002). This is due to the high affinity of critical molecules such as albumin, glutathione, and cysteine for sulfhydryl groups that affects their normal functions (Zalups et al. 1999). Moreover, mercury generates hydrogen peroxide and so contributes to renal failure (Nath et al. 1996).

Melatonin (MEL), the main pineal hormone, is a potent free-radical scavenger that stimulates antioxidant enzymes and maintains mitochondrial functions (Reiter et al. 2004). It has been successfully used in various nephrotoxic models (Stacchiotti et al. 2002; Nava et al. 2003; Parlakpinar et al. 2003) and against ischemia/reperfusion injury (Rodriguez-Reynoso et al. 2004). Remarkably, MEL improves mercury toxicity in the kidney and in other essential organs (Nava et al. 2000; Sener et al. 2003).

In a recent immunohistochemical study in rat kidneys, we showed that $HgCl_2$ induced specific stress proteins that were strictly related to mitochondrial abnormalities (Stacchiotti et al. 2004).

To confirm the preventive efficacy of MEL on mercury nephrotoxicity, we specifically focused on the tubular localization and abundance of three stress proteins (HSP72, GRP75, and MT) and iNOS. For defining the effects of treatment in S3 segment we used electron microscopy, whereas we used ultrastructural morphometry to determine mitochondrial size and density. We hypothesized that if antioxidant MEL was beneficial, stress proteins and iNOS distribution in proximal convoluted and straight tubules and mitochondrial damage would be reduced.

Materials and Methods

Animals

Fifty male adult Sprague Dawley rats (Charles River; Milan, Italy) weighing 230–250 g were housed in a controlled environment (12 h light/12 h dark cycle at 20C, relative humidity 50%) and fed with a standard diet and water ad libitum. All treatments began almost 1 week after arrival. Animals were cared for according to national regulations for the protection of laboratory animals (D.M.116192) and EU regulations (L358/112/18/1986). The Italian Ministry of Health approved all procedures.

Experimental Design

Rats were divided into five groups (10 rats each) and treated as follows: group 1: single IP injection of $HgCl_2$ (Sigma-Aldrich; Milan, Italy) at a nephrotoxic dose 3.5 mg/kg (w/v in 1 ml saline/kg) (Stacchiotti et al. 2003); group 2: single SC injection of MEL (Sigma-Aldrich) at 5 mg/kg (w/v), dissolved in ethanol, and diluted in saline to a final concentration of 5% ethanol (v/v, 50 μl in 1 ml saline/kg) at 5:00 PM to enhance the endogenous increase (Liu and Ng 2000). This

dose was chosen based on a study by Meki and Hussein (2001); group 3: MEL plus $HgCl_2$ at the above doses but MEL administered 30 min before the mercury; group 4: IP injection of sterile 0.9% (w/v in 1 ml/kg) saline; group 5: IP injection 5% ethanol (v/v, 50 μl in 1 ml saline/kg). All animals were killed by cervical dislocation after 24 hr. Kidneys were rapidly extracted and decapsulated in sterile saline and then used as above. A whole kidney for each rat was fixed by immersion in 4% cold paraformaldehyde for 48 hr, dehydrated in a graded series of ethanol, embedded in paraffin wax, and used for immunohistochemistry. The other kidney was partly fixed by immersion in liquid nitrogen and stored at −80C for cryosections and immunoblotting. Finally, a small piece of renal cortex was fixed by immersion in fresh 2.5% glutaraldehyde in 0.1 M PBS, pH 7.4, for 3 hr at 4C for electron microscopy.

Immunohistochemistry

Four-μm-thick sections were collected on poly-L-lysine-coated slides (Sigma; St Louis, MO) and dried overnight at 37C. The various markers were immunohistochemically localized using the ABC–peroxidase method. Microwave oven pretreatment in citrate buffer was used only for HSP72 staining detection as previously reported (Stacchiotti et al. 2001). We tested for the detection of stress proteins monoclonal anti-HSP72 and anti-GRP75 antibodies (StressGene Bioreagents; Ann Arbor, MI) diluted 1:400; for metallothionein, a monoclonal anti-MT antibody (clone E9; DakoCytomation, Milan, Italy) diluted 1:50; polyclonal antibody anti-NOS 2 enzyme (Santa Cruz Biotechnology; Santa Cruz, CA) diluted 1:200, respectively. All incubations of primary antibodies were overnight at 4C except for the MT antibody that was tested for 2.5 hr at room temperature. Both secondary biotinylated antibodies and ABC reaction were applied sequentially and performed according to the commercial kit instructions (Vectastain-Elite; Vector Laboratories, Burlingame, CA). Localization was visualized with DAB and counterstained in Mayer's hematoxylin, dehydrated, and mounted in DPEX (BDH; Milan, Italy). To ensure specificity of the immunostaining, adjacent control sections were subjected to all the above procedures with the exception that primary antibodies were replaced by non-immune goat or horse serum or by absorption with their specific antigenic peptide or fusion protein (StressGene Bioreagents). To exclude incorrect interpretation of the immunostaining due to endogenous biotin (Nayler et al. 1998), we also carried out experiments using the peroxidase–anti-peroxidase detection system but obtained similar patterns. Each set of experiments was done in triplicate and always carried out under the same experimental conditions.

For quantitative analysis of immunostaining intensity in mid-cortical proximal tubules, we blindly computed the integrated optical density (IOD) and measured 10 samples for each experimental group. Digitally fixed images were analyzed at ×200 magnification using an Olympus (Hamburg, Germany) light microscope equipped with an image analyzer (Image Pro Plus; Milan, Italy). IOD was calculated for arbitrary areas (20 arbitrary areas/samples, 1000 × 1500 μm), each sample being the same size. All data were a mean value, and statistical analysis was applied to compare the results from the various experimental groups.

SDS-PAGE and Western Blot Analysis

Whole-tissue homogenates were obtained in PBS for Western blot analysis, and protein levels were observed using the same monoclonal and polyclonal antibodies used for immunohistochemistry. Briefly, 30 μg of lysate supernatant was separated by 10% (w/v) SDS-PAGE at a constant current of 45 mA and transferred onto nitrocellulose membranes. Membranes were incubated overnight with 5% (w/v) milk in 10 mM Tris–HCl (pH 7.4), 150 mM NaCl, 0.05% Tween 20 (TBST) buffer at 4C. After washing with TBST, membranes were incubated with a 1:1000 dilution of anti-iNOS, anti-GRP75, anti-HSP72 antibodies or with a 1:500 dilution for monoclonal anti-MT antibody overnight at room temperature with constant shaking. The filters were then washed and subsequently probed with horseradish peroxidase-conjugated anti-mouse IgG (Santa Cruz Biotechnology) for HSP72, MT, and GRP75 at a dilution of 1:2000 or horseradish peroxidase-conjugated anti-rabbit IgG (Santa Cruz Biotechnology) for iNOS at a dilution of 1:5000. Chemiluminescence detection was made using an Enhanced Chemiluminescence Detection kit (Amersham; Milan, Italy) according to the manufacturer's instructions. Each experiment was repeated three times and densitometrically analyzed after normalization with β-actin running.

Electron Microscopy

The other kidney of each rat was postfixed in 1% (v/v) osmium tetroxide in PBS, dehydrated in ethanol and propylene oxide, and embedded in epoxy araldite resin (Serva; Heidelberg, Germany). Both semithin (1-μm thick) and ultrathin sections (800 nm) were obtained by an ultramicrotome (Ultracut E; Reichert-Jung, Wetzlar, Germany) using glass or diamond blades (Microstar; Huntsville, TX). For microscopic
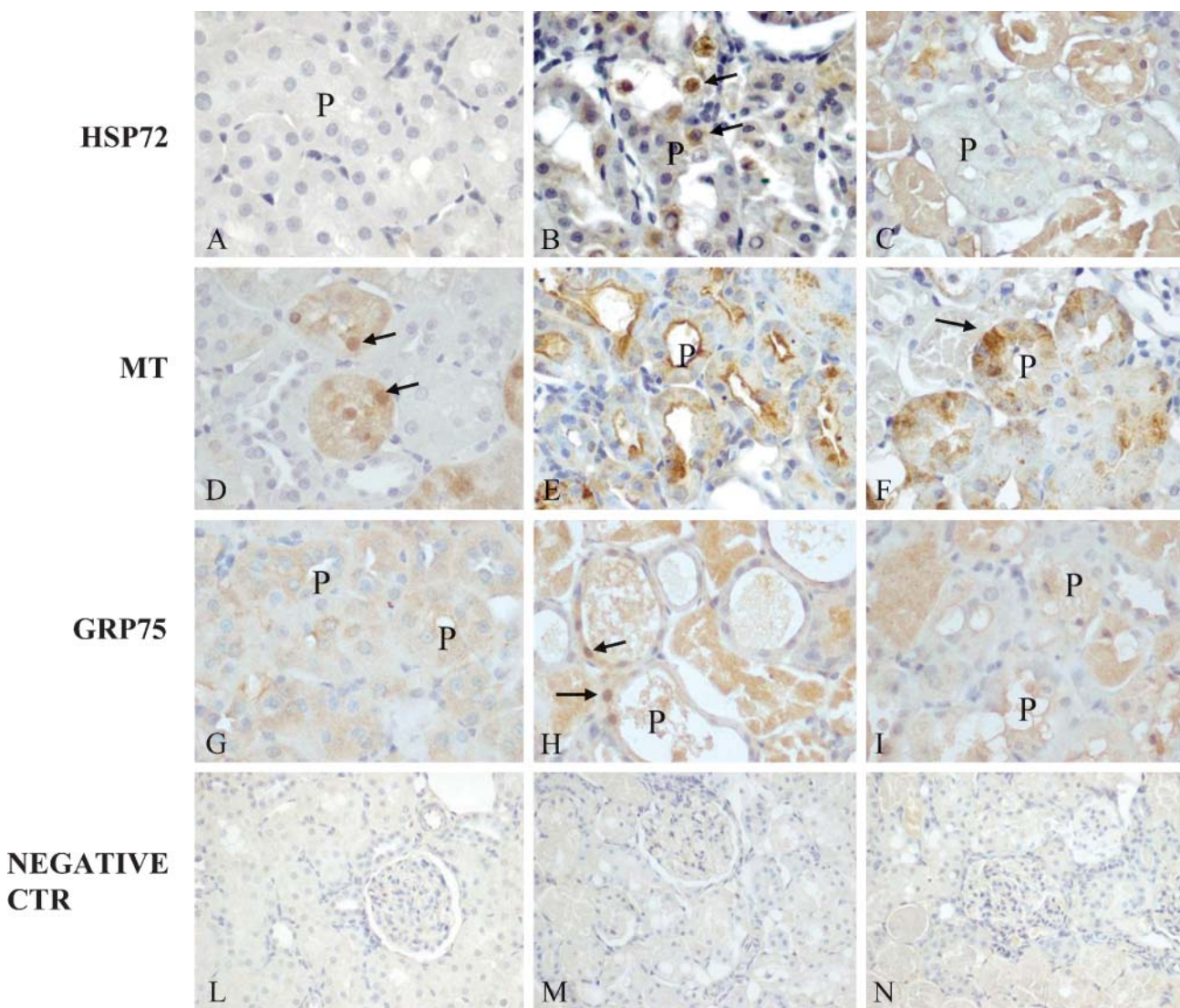

Figure 1 Immunostaining of stress proteins within rat kidneys: HSP72 after melatonin (MEL) **(A)**, mercuric chloride (HgCl₂) **(B)**, and MEL + HgCl₂ **(C)**; metallothionein (MT) after MEL **(D)**, HgCl₂ **(E)**, MEL + HgCl₂ **(F)**; GRP75 after MEL **(G)**, HgCl₂ **(H)**, and MEL + HgCl₂ **(I)**. Negative immunohistochemical control after MEL **(L)**, HgCl₂ **(M)**, MEL + mercuric chloride **(N)**. Nuclear positivity (arrows), proximal tubules (P). Sections were counterstained by Mayer's hematoxylin.

analysis, semithin sections were stained using toluidine blue and ultrathin sections by uranyl acetate and lead citrate solutions. Electron micrographs were taken with a CM10 transmission electron microscope (Philips; Eindhoven, The Netherlands) set at 80 kV.

Morphometric and Statistical Analysis

Data were point-counted from 50 randomly chosen fields of the straight portion of proximal tubules for each group, five from each rat. All counts were made by different investigators unaware of the experimental treatment. Both area fractions ($\mu m^2/\mu m^2$) occupied by mitochondria and numerical density (number/100 μm^2) of the total mitochondria were calculated by point-counting at a final enlargement of $\times 11,700$ as previously described (Stacchiotti et al. 2004). Data are presented as mean $\pm$ SD. Statistical analysis between groups was made by variance analysis (ANOVA) corrected by the Bonferroni test (significant at $p < 0.05$).

Results

Because the data obtained were similar for both the saline- and ethanol-5%-treated groups, we decided to consider them without distinction and to report only the saline group data as the "control group."

All immunohistochemical controls were negative, and representative pictures are shown in Figures 1L–1N.

Stress Protein Distribution

In the corticomedullary junction, HSP72 was barely detectable in the control and after MEL-only administration (Figure 1A). It was also strongly induced in the mercury-treated rats in the nuclei of proximal tubules (Figure 1B) and was maintained in the cytoplasm of disrupted proximal tubules after MEL coadministration (Figure 1C).

MT immunostaining was faint and occasionally nuclear in mid-cortical tubules in control and MEL-only treated groups (Figure 1D) but became intense in the cytoplasm of altered proximal tubules after mercury exposure, often outlining the apical side and the lumen (Figure 1E). After MEL coadministration, the MT pattern was moderate and diffuse in the affected proximal tubules (Figure 1F).

GRP75 signal was faint and basolateral in control and MEL only cortical tubules (Figure 1G), but after mercury exposure, became strong and often translocated into the nuclei (Figure 1H). After MEL supply, there was a moderate signal in the cytoplasm of proximal tubules at the corticomedullary junction (Figure 1I).

iNOS

We also described the immunohistochemical distribution of iNOS in cortical tubules. iNOS immunostaining was almost undetectable in both control and MEL-only-treated rats (Figure 2A). In contrast, after mercury administration, clear iNOS staining was induced in the cytoplasm of proximal tubules (Figure 2B), but after MEL supply its pattern became punctated and faint (Figure 2C).

Quantitative Analysis of the Immunostaining

Digitally acquired fields were computed for each examined marker and expressed as an IOD in Figure 3. Elevated signals were measured in mercury-treated groups with respect to controls in HSP72, GRP75, MT, and iNOS immunostainings. A considerable pattern was estimated for MT immunostaining where the IOD was 23 vs 14, and after MEL supply the staining intensity was statistically different from controls. In contrast, a moderate signal in the mercury-treated group was estimated for HSP72 that persisted also until after the MEL supply. IOD was 13 and after MEL supply was 14.5.

Immunoblotting Analysis of Renal Extracts

In rats treated with HgCl$_2$, the effects of MEL supply on the renal abundance of HSP72 protein are shown in Figure 4, GRP75 and MT in Figure 5, and NOS
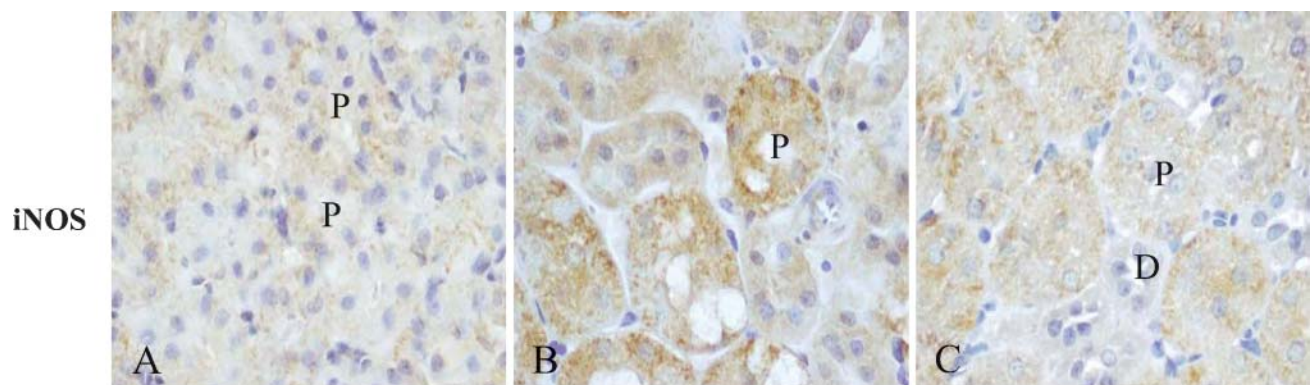

Figure 2 Immunolocalization of inducible nitric oxide synthase (iNOS) within rat kidneys after MEL (**A**), HgCl$_2$ (**B**), and MEL + HgCl$_2$ (**C**). Distal tubules (D); proximal tubules (P). All sections were counterstained by Mayer's hematoxylin.
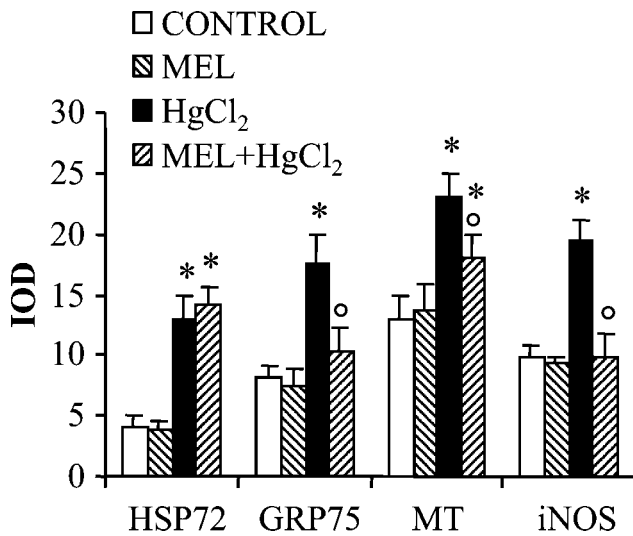
Figure 3 HSP72, GRP75, MT, and iNOS staining intensity in rat proximal tubules. Integrated optical density (IOD) was plotted for each experimental group. Data are expressed as mean ± SD. *$p<0.05$ vs control group, $p<0.05$ vs mercury-treated group.

it is an inducible protein, it became thicker in mercury-treated group and persisted after MEL supply (Figure 4A). For GRP75 and MT, a similar amount was detected in the control and MEL-only-treated groups, whereas after mercury treatment larger bands were detected that decreased after MEL coadministration (Figure 5A). Finally, an iNOS immunoblotting analysis was made: the iNOS band was higher after mercury exposure and lower after MEL supply, very similar to control and MEL-only-treated groups (Figure 6A). Densitometric data representative of immunoblotting analysis are included under their relative bands in Figures 4B, 5B, and 6B.

Ultrastructural and Morphometric Analysis

We clearly analyzed the morphology of the proximal convoluted and straight tubules under different experimental conditions on semithin sections. After MEL intake only, the feature was similar to controls except for clear signs of lysosomes. Nuclei and brush border were well preserved (Figure 7A). In contrast, after HgCl₂ we observed vacuolated cells with disrupted brush border and some mitotic figures (Figure 7B). In MEL + HgCl₂ group, proximal tubular S2–S3 segments were well preserved and displayed a regular brush border (Figure 7C). Ultrastructural features of tubular compartments were also described. Inside the S3 segment of proximal tubules in the mercury-treated
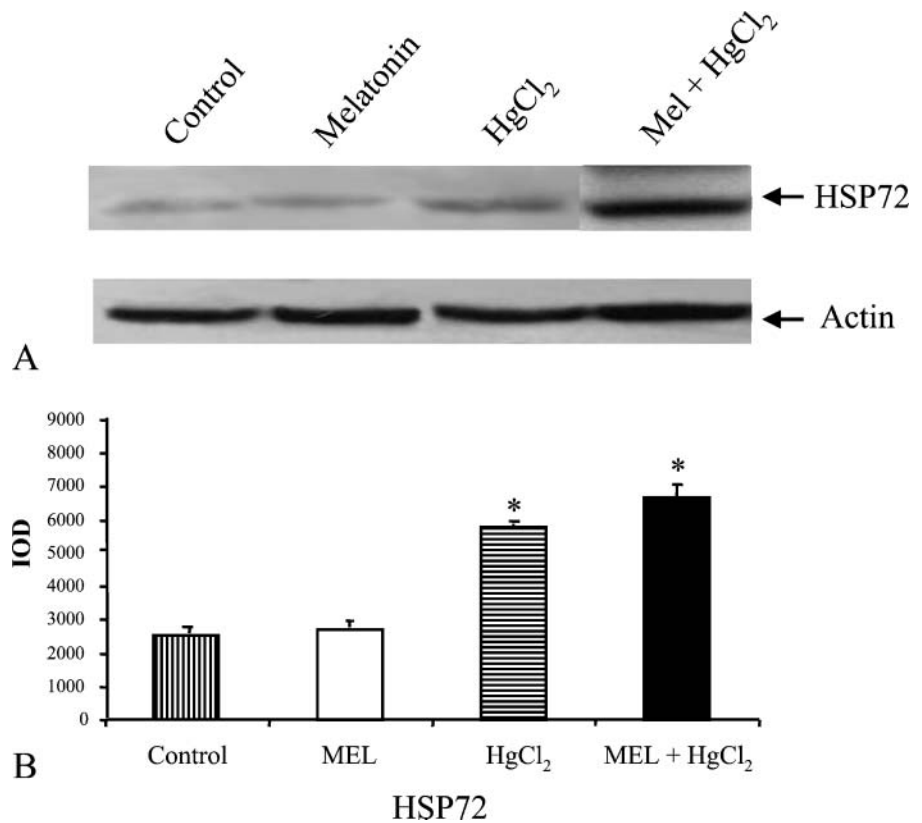
isoforms in Figure 6. Overall amount of these markers was almost in agreement with the immunohistochemical results.

In HSP72 immunoblotting, the band was narrow in control and MEL-only-treated groups. Considering that

Figure 4 Effect of HgCl₂ exposure on HSP72 expression in kidneys from MEL-, HgCl₂-, and MEL + HgCl₂-treated rats. **(A)** Immunoblotting (IB) from controls, MEL, HgCl₂, and MEL + HgCl₂. **(B)** Quantitative analysis of HSP72 expression determined as IOD of IB. *$p<0.05$ vs control.
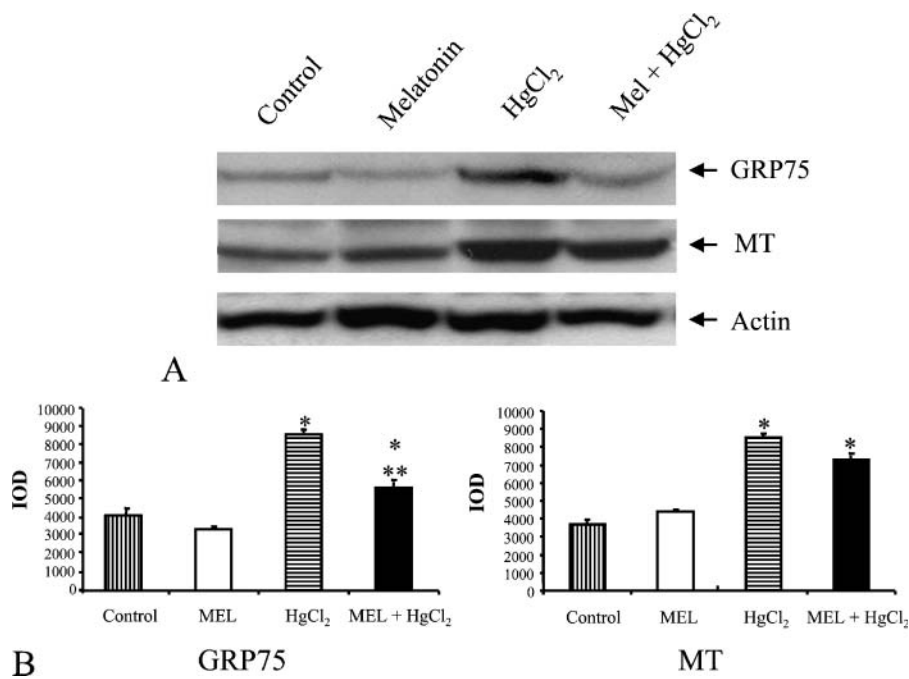
Figure 5 Effect of $HgCl_2$ exposure on GRP75 and MT expression in kidney from MEL-, $HgCl_2$-, and MEL + $HgCl_2$-treated rats. **(A)** IB from controls, MEL, $HgCl_2$, and MEL + $HgCl_2$. **(B)** Quantitative analysis of GRP75 and MT expression determined as IOD of IB. *$p < 0.05$ vs control; **$p < 0.05$ vs $HgCl_2$.

group we observed clear mitochondrial damage (Figure 7D). However, in MEL + mercury group, cell membranes of tubular epithelial cells and major organules such as mitochondria and lysosomes were well preserved (Figure 7E).

Morphometric data on mitochondria in different experimental groups are summarized in Table 1. Total mitochondrial area and density both increased in mercury-exposed rats vs MEL-only-treated rats. However, after MEL pretreatment, all parameters decreased
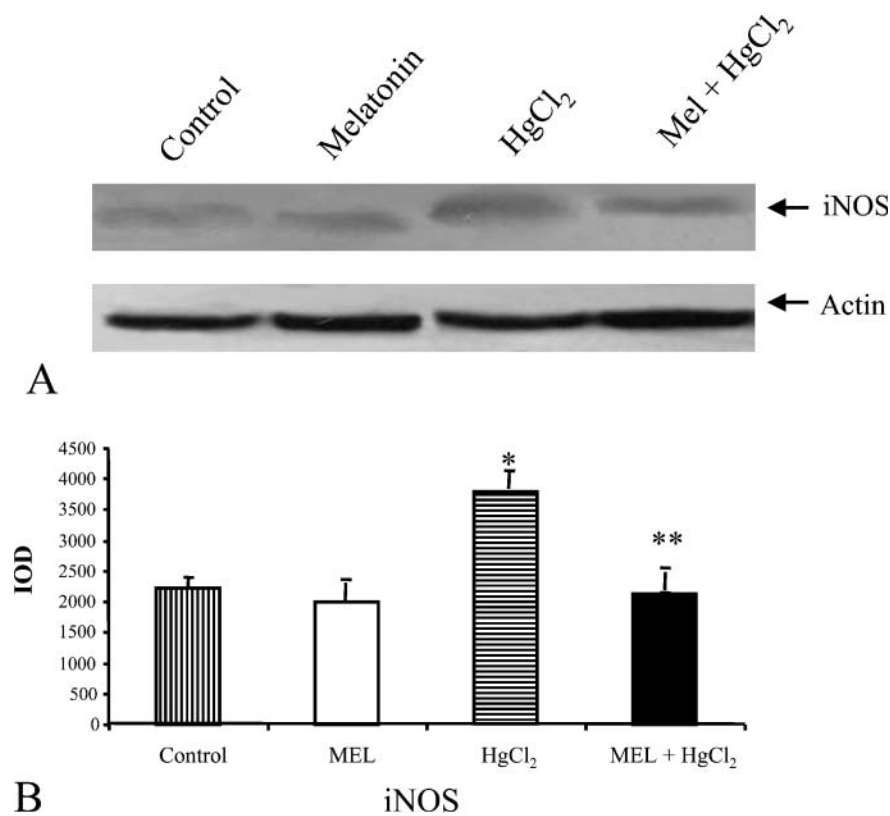

Figure 6 Effect of $HgCl_2$ exposure on iNOS expression in kidney from MEL-, $HgCl_2$-, and MEL + $HgCl_2$-treated rats. **(A)** Immunoblotting (IB) from controls, MEL, $HgCl_2$ and MEL + $HgCl_2$. **(B)** Quantitative analysis of iNOS expression determined as IOD of IB. *$p < 0.05$ vs control; **$p < 0.05$ vs $HgCl_2$.
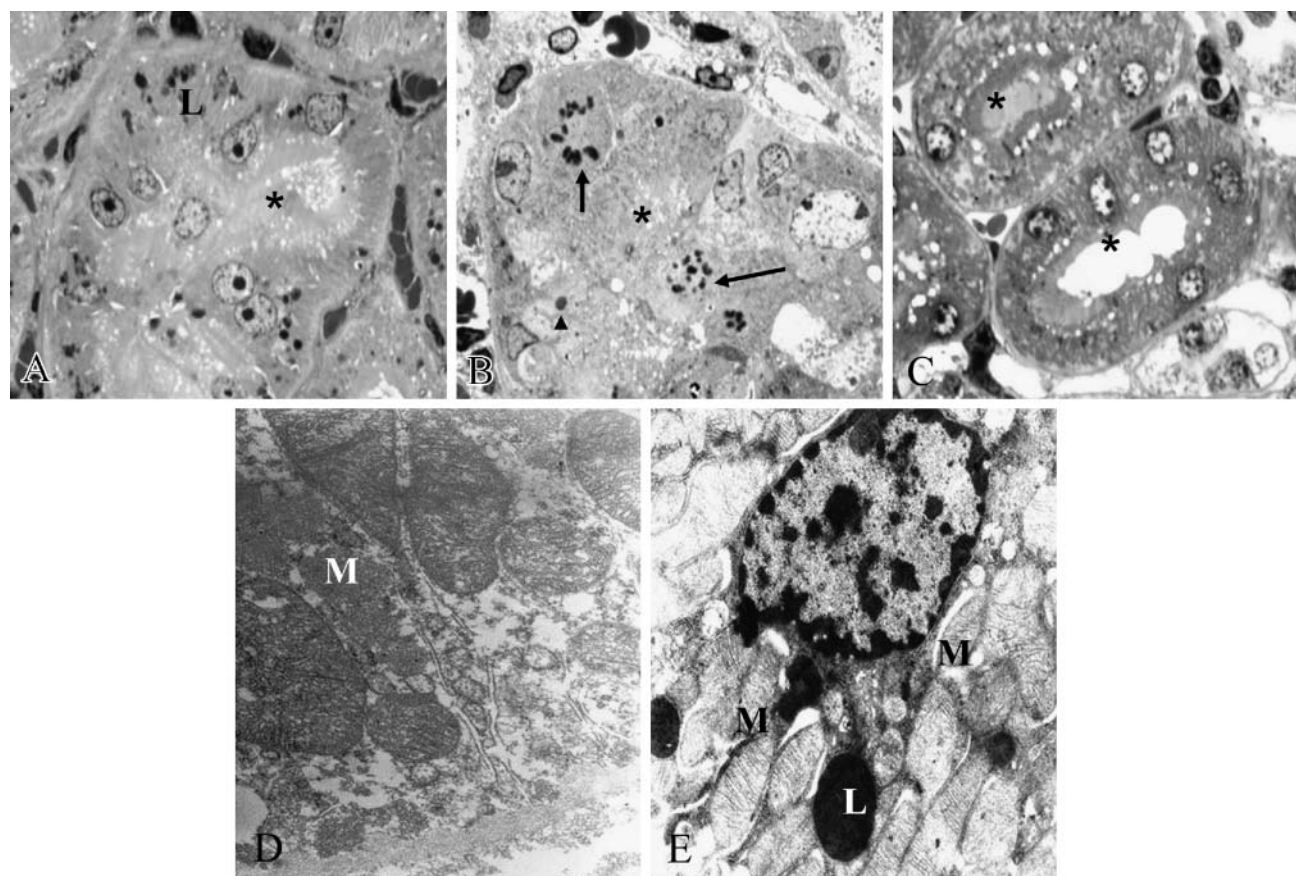
Figure 7 Toluidine-blue-stained semithin sections. Mitotic figures (arrows) and necrotic nucleus (arrowhead) and detached brush border (*) were present in the mercury-treated group (**B**) but were absent in the MEL-treated group (**A**) and after mercury + MEL (**C**). Ultrastructure of straight proximal tubule treated by mercury (**D**) displayed altered mitochondria but recovered after MEL supply (**E**). Lysosome (L), Mitochondria (M).

and, in particular, mitochondrial density was not statistically different from the control groups.

Discussion

HgCl₂ induces acute renal failure in humans and experimental animals (Clarkson 1997) where glomerular hemodynamics and, more specifically, proximal tubules (Zalups 2000) are affected. The pathogenic mechanism also includes oxidative damage; therefore, antioxidant intake could attenuate or prevent this toxicity. Many compounds have been reported to improve mercury-induced renal damage (Girardi and Elias 1991; Sang-

Kyung et al. 2004). In particular, MEL, the main pineal neurohormone, improves nephrotoxicity if administered before and/or after the mercury (Nava et al. 2000; Sener et al. 2003).

Stress proteins are universally conserved proteins that are a reliable index of repair in injured renal cells (Van de Water et al. 2006). By virtue of their molecular chaperone property, they protect cells by binding to other essential proteins or organules, thus preventing denaturation and malfolding caused by toxic metals. Nitric oxide is a gas generated from L-arginine by NOS that functions as an intercellular messenger in renal injury and inflammation (Michel and Feron 1997).

Table 1 Ultrastructural morphometric data on proximal tubules exposed to mercuric chloride and melatonin

Treatments (n=10 rats/group)	A Melatonin (5 mg/kg)	B Mercuric chloride (3.5 mg/kg)	C Mercuric chloride + melatonin
Intact mitochondria area (μm²/μm²)	0.08 ± 0.02	0.06 ± 0.01	0.08 ± 0.02
Total mitochondria* area (μm²/μm²)	0.08 ± 0.02	0.16 ± 0.02[a,c]	0.12 ± 0.02[a,b]
Total mitochondria* density (number/100 μm²)	73.6 ± 3.8	84.3 ± 3.4[a,c]	74.8 ± 3.4[b]

[a,b,c]Indicate significant value vs respective group ($p < 0.05$).
*Total mitochondria comprise both intact and broken cristae mitochondria.
Data are expressed as mean ± SD; saline-treated group was similar to melatonin-only group and thus omitted.

iNOS exacerbates renal oxidative damage (Chatterjee et al. 2002). We therefore focused on the effects of MEL on tubular expression of three stress proteins (HSP72, GRP75, and MT) and iNOS in rats treated with a nephrotoxic dose of $HgCl_2$ at 3.5 mg/kg. Because it was reported that, after similar doses, toxicological parameters such as malondialdheyde and blood urea nitrogen peaked at 24 hr, we chose this time to test MEL pretreatment (Girardi et al. 1996; Huang et al. 1996).

The main findings of our study were as follows: 1) MEL pretreatment reduced stress proteins and iNOS expressions within proximal convoluted and straight tubules affected by mercury; 2) MEL improved tubular morphology, in particular the mitochondrial shape and density within S3 segment, the main mercury target.

HSP72, a cytoplasmic-inducible protein, enhanced with the progression of mercury nephrotoxicity (Goering et al. 2000). Hg^{2+} ions directly activate hsp70 promoter in HeLa cells at non-cytotoxic doses (Ait-Aissa et al. 2000). Remarkably, the nuclear HSP72 pattern reported here could be a sign of a recent transcriptional activity to aid kidney recovery from mercury damage. GRP75, a mitochondrial chaperone in the inner mitochondrial matrix, is involved in the refolding of oxidative enzymes (Mitsumoto et al. 2002). Kaul et al. (1997) reported that it migrates into the nuclei after cell proliferation. Enhanced GRP75 signal could be a cytoprotective reaction against mercury-induced mitochondrial damage (Stacchiotti et al. 2004), whereas its reduction after MEL supply could be associated with the recovery of respiratory enzymes (Acuna-Castroviejo et al. 2003; Leon et al. 2004). MT has been previously reported in the kidney and liver after mercury treatment (Zalups and Koropatnick 2000; Sanchez Reus et al. 2003). Its presence in proximal convoluted tubules correlates with Hg^{2+} deposition and transport (Tandon et al. 2001), whereas its diffuse pattern after MEL pretreatment could be due to the lower transport efficiency of the metal.

Another important marker of tubular impairment that greatly influences acute renal failure is iNOS (Goligorsky et al. 2002). In this study, clear iNOS signals in proximal convoluted tubules after mercury treatment became very faint after MEL supply. A similar trend was indicated by Rodriguez-Reynoso et al. (2004) who demonstrated a direct inhibitory effect of MEL on iNOS during renal ischemia/reperfusion.

In conclusion, we confirmed that MEL is beneficial against experimental $HgCl_2$ nephrotoxicity. Its antioxidant effect is corroborated by reduced expression of a mitochondrial chaperone, GRP75, and iNOS in rat proximal convoluted tubules. Remarkably, the tubular persistence of stress proteins such as HSP72 and MT might be a compensatory reaction to speed up recovery. In addition, maintenance of regular morphology and mitochondrial size and density in S3 segments were shown by ultrastructure and morphometry after MEL supply. These results are encouraging although further studies are needed to clarify the mechanism of MEL in acute toxic renal failure before it can be applied as a preventive tool.

Literature Cited

Acuna-Castroviejo D, Escames G, Leon J, Carazo A, Khaldy H (2003) Mitochondrial regulation by melatonin and its metabolites. Adv Exp Med Biol 527:549–557

Ait-Aissa S, Porcher J, Arrigo A, Lambre C (2000) Activation of the hsp70 promoter by environmental inorganic and organic chemicals: relationships with cytotoxicity and lipophilicity. Toxicology 145:147–157

Aleo M, Morandini F, Bettoni F, Tanganelli S, Vezzola A, Giuliani R, Steimberg N, et al. (2002) Antioxidant potential and gap junction-mediated intercellular communication as early biological markers of mercuric chloride toxicity in the MDCK cell line. Toxicol In Vitro 16:457–465

Beck F, Neuhofer W, Muller E (2000) Molecular chaperones in the kidney: distribution, putative roles and regulation. Am J Physiol Renal Physiol 279:F203–215

Chatterjee P, Patel N, Kvale E, Cuzzocrea S, Brown P, Stewart K, Mota-Filipe H, et al. (2002) Inhibition of inducible nitric oxide synthase reduces renal ischemia-reperfusion injury. Kidney Int 61:862–871

Clarkson T (1997) The toxicology of mercury. Crit Rev Clin Lab Sci 34:369–403

Girardi G, Elias M (1991) Effectiveness of N-acetylcysteine in protecting against mercuric chloride-induced nephrotoxicity. Toxicology 67:155–164

Girardi G, Saball D, Salvarrey M, Elias M (1996) Glomerular compromise in mercuric chloride-induced nephrotoxicity. J Biochem Toxicol 11:189–196

Goering PL, Fisher BR, Noren BT, Papacostantinou A, Rojko JL, Marler RJ (2000) Mercury induces regional and cell-specific stress protein expression in rat kidney. Toxicol Sci 53:447–457

Goligorsky M, Brodsky S, Noiri E (2002) Nitric oxide in acute renal failure: NOS versus NOS. Kidney Int 61:855–861

Huang Y, Cheng S, Lin T (1996) Lipid peroxidation in rats administered with mercuric chloride. Biol Trace Elem Res 52:193–206

Jarry A, Renaudin K, Denis M, Robard M, Buffin-Meyer B, Karam G, Buzelin F, et al. (2003) Expression of NOS1 and soluble guanylyl cyclase by human kidney epithelial cells: morphological evidence for an autocrine/paracrine action of nitric oxide. Kidney Int 64: 170–180

Kaul S, Matsui M, Takano S, Sugihara T, Mitsui Y, Wadhawa R (1997) Expression analysis of mortalin, a unique member of the Hsp70 family of proteins, in rat tissues. Exp Cell Res 232:56–63

Kone B (2004) Nitric oxide synthesis in the kidney: isoforms, biosynthesis, and functions in health. Semin Nephrol 24:299–315

Kultz D (2005) Molecular and evolutionary basis of the cellular stress response. Annu Rev Physiol 67:225–257

Leon J, Acuna-Castroviejo D, Sainz R, Mayo J, Tan D, Reiter R (2004) Melatonin and mitochondrial function. Life Sci 75:765–790

Liu F, Ng T (2000) Effect of pineal indoles on activities of the antioxidant defense enzymes superoxide dismutase, catalase, and

glutathione reductase, and levels of reduced and oxidized glutathione in rat tissues. Biochem Cell Biol 78:447–453

Mallouk Y, Vayssier-Taussat M, Bonventre JV, Polla BS (1999) Heat shock protein 70 and ATP as partners in cell homeostasis. Int J Mol Med 4:463–474

Meki A, Hussein A (2001) Melatonin reduces oxidative stress induced by ochratoxin A in rat liver and kidney. Comp Biochem Physiol C Toxicol Pharmacol 130:305–313

Michel T, Feron O (1997) Nitric oxide synthase: which, where, how, and why? J Clin Invest 100:2146–2152

Mitsumoto A, Takeuchi A, Okawa K, Nakagawa Y (2002) A subset of newly synthesized polypeptides in mitochondria from human endothelial cells exposed to hydroperoxide stress. Free Radic Biol Med 32:22–37

Nath K, Croatt A, Likely S, Beherens T, Warden D (1996) Renal oxidant injury and oxidant response induced by mercury. Kidney Int 50:1032–1043

Nava M, Quiroz Y, Vaziri N, Rodriguez-Iturbe B (2003) Melatonin reduces renal interstitial inflammation and improves hypertension in spontaneously hypertensive rats. Am J Physiol Renal Physiol 284:F447–454

Nava M, Romero F, Quiroz Y, Parra G, Bonet L, Rodriguez-Iturbe B (2000) Melatonin attenuation of acute renal failure and oxidative stress induced by mercuric chloride in rats. Am J Physiol Renal Physiol 279:F910–918

Nayler SJ, Goetsch S, Cooper K (1998) Biotin inclusions: a potential pitfall in immunohistochemistry. Histopathology 33:87–94

Parlakpinar H, Ozer M, Sahna E, Vardi N, Cigremis Y, Acet A (2003) Amikacin-induced acute renal injury in rats: protective role of melatonin. J Pineal Res 35:85–90

Reiter R, Tan D, Gitto E, Sainz R, Mayo J, Leon J, Manchester L, Vijayalaxmi, Kilic E, Kilic U (2004) Pharmacological utility of melatonin in reducing oxidative cellular and molecular damage. Pol J Pharmacol 56:159–170

Rodriguez-Reynoso S, Leal C, Portilla-de Buen E, Castillo J, Ramos-Solano F (2004) Melatonin ameliorates renal ischemia/reperfusion injury. J Surg Res 116:242–247

Sanchez Reus I, Bando I, Andres D, Cascales M (2003) Relationship between expression of HSP70 and metallothionein and oxidative stress during mercury chloride induced acute liver injury in rats. Biochem Mol Toxicol 17:161–168

Sang-Kyung J, Hu X, Yuen P, Aslamkhan A, Pritchard J, Dear J, Star R (2004) Delayed DMSO administration protects the kidney from mercuric chloride-induced injury. J Am Soc Nephrol 15:2648–2654

Sato M, Kondoh M (2002) Recent studies on metallothionein: protection against toxicity of heavy metals and oxygen free radicals. Tohoku J Exp Med 196:9–22

Satoh M, Nishimura N, Kanayama Y, Naganuma A, Suzuki T, Tohyama C (1997) Enhanced renal toxicity by inorganic mercury in metallothionein-null mice. J Pharmacol Exp Ther 283:1529–1533

Sener G, Sehirli AO, Ayanoglu-Dulger G (2003) Melatonin protects against mercury(II)-induced oxidative tissue damage in rats. Pharmacol Toxicol 93:290–296

Shimojo N, Kumagai Y, Nagafune J (2002) Differences between kidney and liver in decreased manganese superoxide dismutase activity caused by exposure of mice to mercuric chloride. Arch Toxicol 76:383–387

Stacchiotti A, Borsani E, Rodella L, Rezzani R, Bianchi R, Lavazza A (2003) Dose-dependent mercuric chloride tubular injury in rat kidney. Ultrastruct Pathol 27:253–259

Stacchiotti A, Lavazza A, Rezzani R, Borsani E, Rodella L, Bianchi R (2004) Mercuric chloride-induced alterations in stress protein distribution in rat kidney. Histol Histopathol 19:1209–1218

Stacchiotti A, Rezzani R, Angoscini P, Corsetti G, Bianchi R (2001) Distribution of heat shock proteins in kidneys of rats after immunosuppressive treatment with cyclosporine A. Acta Histochem 103:167–177

Stacchiotti A, Rezzani R, Angoscini P, Rodella L, Bianchi R (2002) Small heat shock proteins expression in rat kidney treated with cyclosporine A alone and combined with melatonin. Histochem J 34:305–312

Tandon S, Singh S, Prasad S, Mathur N (2001) Hepatic and renal metallothionein induction by an oral equimolecular dose of zinc, cadmium or mercury in mice. Food Chem Toxicol 39:571–577

van de Water B, de Graauw M, Le Devedec S, Alderliesten M (2006) Cellular stress responses and molecular mechanisms of nephrotoxicity. Toxicol Lett 162:83–93

Van Vleet T, Schnellmann R (2003) Toxic nephropathy: environmental chemicals. Semin Nephrol 23:500–508

Wadhwa R, Taira K, Kaul SC (2002) An Hsp70 family chaperone, mortalin/mthsp70/PBP74/Grp75: what, when, and where? Cell Stress Chaperones 7:309–316

Yoshida M, Watanabe C, Satoh M, Yasutake A, Sawada M, Ohtsuka Y, Akama Y, et al. (2004) Susceptibility of metallothionein-null mice to the behavioral alterations caused by exposure to mercury vapor at human-relevant concentration. Toxicol Sci 80:69–73

Zalups R (2000) Molecular interactions with mercury in the kidney. Pharmacol Rev 52:113–143

Zalups R, Barfuss D, Lash L (1999) Relationship between alterations in glutathione metabolism and the disposition of inorganic mercury in rats: effects of biliary ligation and chemically induced modulation of glutathione status. Chem Biol Interact 123:171–195

Zalups R, Koropatnick J (2000) Temporal changes in metallothionein gene transcription in rat kidney and liver: relationship to content of mercury and metallothionein protein. J Pharmacol Exp Ther 295:74–82